World Academy of Science, Engineering and Technology
International Journal of Electrical and Computer Engineering
Vol:4, No:5, 2010

# Pattern Recognition of Partial Discharge by Using Simplified Fuzzy ARTMAP

S. Boonpoke and B. Marungsri*



***Abstract*—** This paper presents the effectiveness of artificial intelligent technique to apply for pattern recognition and classification of Partial Discharge (PD). Characteristics of PD signal for pattern recognition and classification are computed from the relation of the voltage phase angle, the discharge magnitude and the repeated existing of partial discharges by using statistical and fractal methods. The simplified fuzzy ARTMAP (SFAM) is used for pattern recognition and classification as artificial intelligent technique. PDs quantities, 13 parameters from statistical method and fractal method results, are inputted to Simplified Fuzzy ARTMAP to train system for pattern recognition and classification. The results confirm the effectiveness of purpose technique.

***Keywords*—**Partial discharges, PD Pattern recognition, PD Classification, Artificial intelligent, Simplified Fuzzy ARTMAP, .

## I. Introduction

PARTIAL discharge (PD) is electrical discharges that do not completely bridge the distance between two electrodes under high voltage stress. Partial discharges are small electrical sparks that occur within the electric insulation of electrical equipment. Although the magnitude of such discharges is usually small, it cause progressive deterioration and may lead to ultimate failure [1],[2].

Partial discharge is one of the factors that could lead to failure of electrical equipment. Also, partial discharges could destroy insulation and cause ageing of insulation. Occurrence of partial discharge in electrical insulation is always associated with emission of several signals (i.e. electrical signal, acoustic pulses and chemical reactions).

Up to now, artificial intelligent techniques have been adopted to many applications in electrical engineering field[3]–[8]. The objective of this work is applying an artificial intelligent technique, simplified fuzzy ARTMAP (SFAM), to recognize the pattern of partial discharge. In this paper, classification of partial discharge is given in Section II, characteristics of partial discharge quantities are given in Section III, partial discharge measurement techniques are detailed in Section IV and following with detail of SFAM is given in Section IV. In addition, experimental results and PDs pattern recognition are illustrated in Section V and Section VI, respectively. Finally, discussion and conclusion are given.

S. Boonpoke is with Suranaree University of Technology, Nakhon Ratchasima, 30000, THAILAND (e-mail: suphachai_eesut@ hotmail.com).

* B. Marungsri is with Suranaree University of Technology, Nakhon Ratchasima, 30000, THAILAND (corresponding author, phone: +66 4422 4366; fax: +66 4422 4601; e-mail: bmshvee@ sut.ac.th).

## II. Classification of Partial Discharges

Partial discharges are divided into four types: (i) internal discharges, (ii) corona discharges, (iii) surface discharges and (iv) discharges in electrical trees [1],[9].

### *A. Internal discharges*

Internal discharges occur in inclusions of low dielectric strength. These discharges usually occur in gas–filled cavities, but oil – filled cavities can also break down and cause gaseous discharges afterwards. Internal discharges are capable of degrading the insulation depends on the field strength, the kind of material and the discharges magnitude. (Fig. 1.a)

### *B. Corona discharges*

Corona discharges occur at sharp points in the electrical field. These discharges may occur in gases and in liquids. They occur usually at the high-voltage side, but at sharp edges at earth potential, or even at half- way the electrodes also may cause corona discharges. (Fig. 1.b)

### *C. Surface discharges*

Surface discharges may occur in gases or in oil if there is a strong stress component parallel to the dielectric surface. These discharges are known to cause deterioration of dielectrics by heating the dielectric boundary, through charges trapped in the surface and through the formation of chemicals such as nitric acid and ozone. (Fig. 1.c)

### *D. Discharges by electrical treeing*

Electrical trees can start from defects in the solid insulation. After treeing has started a hollow stem and several branches are generated. (Fig. 1.d)

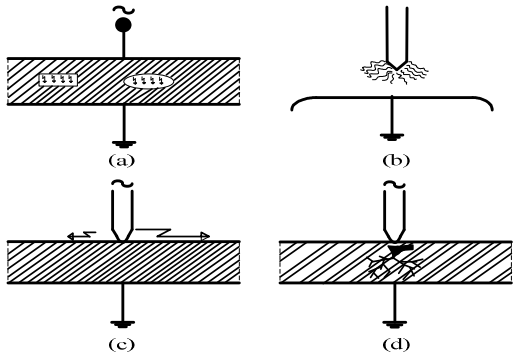


Fig. 1. Types of Partial Discharges.

## III. Partial Discharges Detection Techniques

Occurrence of PDs in electrical insulation is always associated with emission of several signal electrical signal, acoustic signal and chemical reactions, i.e. heat, sound, light and gas. The method to detection PD signal can be grouped into three categories, based on the PD manifestation that they measure: chemical, acoustic and electrical detections [9].

Chemical detection: One of the consequences of PDs is chemical change of material. (i.e. oil, solid and gas)[10].

Acoustic detection of PD is based on the detection of the mechanical waves propagated from the discharge site to the surrounding medium. Acoustic detection has been widely used in diagnostics of transformers. The primary advantage of using acoustic detection is position information is readily available from acoustic systems using sensors at multiple locations [11]-[13].

Electrical partial discharges detection methods are based on the appearance of a partial discharges pulse at the terminals of a test object. Electrical detection includes two methods: Pulse Current Method and Ultra High Frequency Method (UHF).

Pulse Current Method: This method gets the apparent charge by detecting the PD current in detecting impedance [9],[14]. Pulse Current Method is easy for quantitative measurement and it has high sensitivity.

Ultra High Frequency Method (UHF): UHF detection which is based on the detection of electrical resonance at ultrahigh frequencies can be applied to realize not only the phenomena but also the location of a PD source [15] – [17].

In this paper, electrical detection technique was adopted to measure partial discharges signal. Most partial discharges detection systems are integrated into the test circuit in accordance with schemes show in Fig. 2.

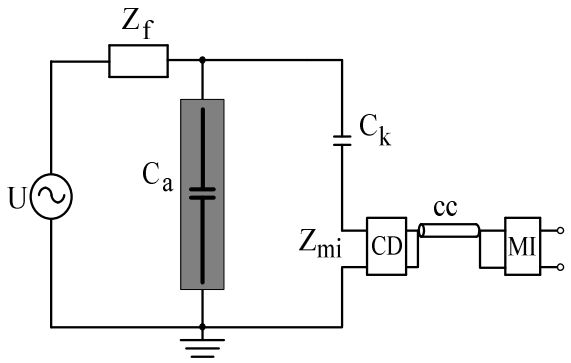


Fig. 2. Basic partial discharge test circuit

U high-voltage supply
$Z_{mi}$ input impedance of measuring system
CC connecting cable
$C_a$ test object
$C_k$ coupling capacitor
CD coupling device
MI measuring instrument
$Z_f$ filter

The coupling capacitor, $C_k$, shall be of low inductance design and should exhibit a sufficiently low level of partial discharges at the specified test voltage to allow the measurement of the specified partial discharge magnitude.

The high voltage supply shall have sufficiently low level of background noise to allow the specified partial discharge magnitude to be measured at the specified test voltage.

## IV. Characteristics of Partial Discharges

Characteristics of partial discharges for pattern recognition and classification are computed from the relation of the voltage phase angle, the discharge magnitude and the repeated existing of partial discharges by using statistical and fractal methods [1],[9],[14].

### A. Basic quantities

Quantities of the first group will be termed basic quantities and for their registration the momentary values of the test voltage and the discharge signal are registered. The electrical activity of partial discharges can be represented by two independent quantities:

(a) Discharge magnitude
(b) Discharge timing

### B. Deduced quantities

Quantities of the second group will be termed deduced quantities. For their registration the basic quantities have to be observed during a time span that is much longer than the duration of one voltage cycle. These quantities can be analyzed as a function of time and as a function of the phase angle.

The quantities as function of time describe the changes of the basic quantities in the course of time.

The quantities as function of the phase angle represent the recurrence of partial discharges related to their phase angle. The voltage cycle is divided into phase window representing the angle axis (0–360°). The four quantities can be determines in each phase window.

1. The sum of the discharge magnitudes observed in one phase window (discharge amount).
2. The number of discharges observed in one phase window (pulse count).
3. The average value of discharges observed in one phase (mean pulse height).
4. The maximum value of discharge observed in one phase window (maximum pulse height).

### C. Statistical operators

Quantities of the third group will be termed as statistical operators. They provide the analysis of some the deduced quantities from the second group.

The pulse count distribution $H_n(\varphi)$ represents the number of the observed discharges in each phase window as a function of the phase angle.

The mean pulse height distribution $H_{qn}(\varphi)$ represents the average amplitude in each phase window as a function of the

phase angle. $H_{qn}(\varphi)$ is derived from the total discharge amount in each phase window divided by the number of discharges in the same phase window.

In the case of a single defect, discharge quantities can be fairly well described by a normal distribution process. Therefore to get a better evaluation of $H_{qn}(\varphi)$ and $H_n(\varphi)$ quantities, several statistical parameters can be used. They are here termed as statistical operators. For a discrete distribution function, $f(x)$, let's

$$f(x) = P(X = x_i) = p_i \tag{1}$$

where P is the probability: $x_i$ is the discrete value: $p_i$ is the probability value for $x_i$. The following moments $u_k$ of a distribution can be defined:

$$u_k = \sum (x_i - a)^k \cdot p_i \tag{2}$$

First moment: $u$ - mean value of a distribution; k=1, a=0

$$u = \sum x_i \cdot p_i \tag{3}$$

Second moment: $\sigma^2$ - variance value of a distribution; k=2, a= $u$

$$\sigma^2 = \sum (x_i - u)^2 \cdot p_i \tag{4}$$

Third moment: skewness $S_k$ - indicator of the asymmetry of a distribution as compared to a normal distribution; k=3, a = $u$

$$S_k = \sum \frac{(x_i - u)^3 \cdot p_i}{\sigma^3} \tag{5}$$

Fourth moment: kurtosis $K_u$ - indicator of the sharpness of a distribution as compared to a normal distribution; k=4, a = $u$

$$Ku = \sum \frac{(x_i - u)^4 \cdot p_i}{\sigma^4} - 3 \tag{6}$$

The third moment and the fourth moment about the mean are significant with respect to the shape of the distribution.

The skewness, $Sk$, indicates the asymmetry of the distribution. $Sk$ will be zero for asymmetric distribution, positive when the distribution is asymmetric to the left and negative when the distribution is asymmetric to the right.

The kurtosis, $Ku$, indicates the degree of sharpness of the distribution. Kurtosis $Ku$ will be zero for a normal distribution. For a sharper then normal distribution $Ku$ is positive, and if the distribution is flatter than a normal distribution the $Ku$ is negative.

The discharges during a voltage cycle occur in two sequences. For each half of the voltage cycle separate discharge patterns can be found. Thus, the $H_{qn}(\varphi)$ and $H_n(\varphi)$ quantities are characterized by two distributions. For the positive half of the voltage cycle $H^+_{qn}(\varphi)$, $H^+_n(\varphi)$ and for the negative half of the voltage cycle $H^-_{qn}(\varphi)$, $H^-_n(\varphi)$.

Both the $H_{qn}(\varphi)$ and $H_n(\varphi)$ quantities can be described by two skewness, $Sk^+$, $Sk^-$ and two kurtosis $Ku^+, Ku^-$. The distributions $H_{qn}(\varphi)$ and $H_n(\varphi)$ are also characterized by their mean value, their inception phase and the number of peaks. Therefore more statistical parameters can be defined, enabling us to compare the mean value, the inception phase and the number of peaks in the both positive and the negative half of the voltage cycle. The distributions $H_{qn}(\varphi)$ and $H_n(\varphi)$ both positive and negative half of the voltage cycle the following statistical operators have been introduced by discharge asymmetry, $Q$, as the quotient of the mean discharge level in the positive and in the negative half of the voltage cycle.

$$Q = \frac{Q_s^- / N_q^-}{Q_s^+ / N_q^+} \tag{7}$$

The cross-correlation factor *cc*, the formula is used to calculate the cross-correlation factor cc:

$$cc = \frac{\sum x_i y_i - \sum x_i \sum y_i / n}{\sqrt{\left[\sum x_i^2 - \left(\sum x_i\right)^2 / n\right]\left[\sum y_i^2 - \left(\sum y_i\right)^2 / n\right]}} \tag{8}$$

The modified cross-correlation factor, *mcc*, to evaluate the difference between discharge patterns in the positive and the negative half of the voltage cycle is given in (9).

$$mcc = Q \cdot cc \tag{9}$$

## V. Simplified Fuzzy ARTMAP

Adaptive Resonance Theory (ART) was invented by Grossberg, in 1976, as a theory of human cognitive information processing [18]. Carpenter and Grossberg introduced the ART family in the form of a wide variety of supervised and unsupervised NNs [19]–[22]. The most advanced model of the ART family, fuzzy ARTMAP (FAM), could handle both binary and analogue data in a supervised manner [23]. The main drawback to the ART family networks, which prevented others from using them, was their intricacy: the inventors had introduced complicated architectures for their networks instead of presenting them as simple algorithms. This problem later was recognized by the inventors and they presented modified model or simplified model of ART family networks [24],[25].

Originally, ART networks were defined in terms of differential equations, but in practice they are implemented using approximations or analytical solutions to these equations, in the limit. ART networks have their own special terminology. The main idea of unsupervised ART networks is as follows:

(1) Find the nearest cluster prototype that 'resonates' with the input pattern.

(2) Update this cluster prototype to be closer to the input.

The simplified fuzzy ARTMAP (SFAM) was developed by removing redundancies. Details are illustrated in [25]. So, the SFAM is much faster than the FAM and easier to understand and simulate. However, it should be made clear that the SFAM can be used only for classification. The SFAM is essentially a two layer net containing an input and an output layer. Fig. 3 illustrates the architecture of simplified fuzzy ARTMAP.

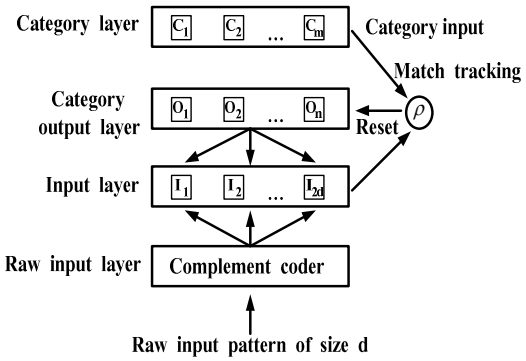


Fig. 3. Architecture of SFAM Network

The main idea of SFAM is as follows[25]:

(1) Find the nearest subclass prototype that 'resonates' with the input pattern (winner).

(2) If the labels of the subclass and the input pattern match, update the prototype to be closer to the input pattern.

(3) Otherwise, reset the winner, temporarily increase the resonance threshold (*r*), and try the next winner.

(4) If the winner is uncommitted, create a new subclass (assign the input vector to be the prototype pattern of the winner, and label it as the class label of the input).

The input to the network flows through the complement coder where the input string is stretched to double the size by adding its complement also. The complement coded input then flows into the input layer and remains there. Weights (*w*) from each of the output category nodes flow down to the input layer. The category layer merely holds the names of the M number of categories that the network has to learn. Vigilance parameter and match tracking are mechanisms of the network architecture which are primarily employed for network training.

$\rho$ is the vigilance parameter which can range from 0 to 1. It controls the granularity of the output node encoding. Thus, while high vigilance values makes the output node much fussier during pattern encoding, low vigilance renders the output node to be liberal during the encoding of patterns.

The match tracking mechanism of the network is responsible for the adjustment of vigilance values. Thus, an error occurs in the training phase during the classification of patterns.

The SFAM algorithm is as follows [25]:

(1) Set the vigilance factor equal to its baseline value :

$$\rho = \overline{\rho} \tag{10}$$

(2) Insert input, and calculate second layer activities:

$$T_j(I) = \frac{|I \wedge w_j|}{\alpha + |w_j|} \quad \text{for } j = 1,\ldots, N\text{-}19 \tag{11}$$

and for the uncommitted neuron: $T_N = T_0$

(3) Find the winner

$$J = \arg\left[\underset{j}{Max}(T_j)\right] \tag{12}$$

If the winner neuron is uncommitted, go to step 7.

(4) Check the resonance condition, i.e. if the input is similar enough to the winner's prototype:

$$\frac{|I \wedge w_j|}{|I|} = \frac{|I \wedge w_j|}{M} \geq \rho \tag{13}$$

If this condition is fulfilled, go to step 5.

If this condition is not fulfilled, reset the winner ($T_j$ = -1), go to the step 3, and check the next winner.

(5) If the class label of the winner matches with the class label of input, update the prototype pattern to be closer to the input pattern:

$$w_j^{(new)} = \beta(I \wedge w_j^{(old)}) + (1-\beta)w_j^{(old)} \tag{14}$$

and go to step 9, otherwise reset the winner ($T_j$ = -1), temporarily increase the vigilance factor so as to violate the condition of Equation (9), i.e. set $\rho$ equal to :

$$\rho = \frac{|I \wedge w_j|}{M} + \varepsilon \tag{15}$$

(where $\varepsilon$ is a small positive number, i.e. $\varepsilon \approx 0.001$).

(6) If $\rho > 1$, terminate the training for this input pattern in the current epoch (data mismatch), and go to step 9, otherwise go to step 3, and try the next winner.

(7) Create a new subclass, i.e. assign the input vector as the prototype pattern of the winner neuron:

$$w_N = I \tag{16}$$

and set the class label of the winner neuron to be as the class label of input pattern.

(8) Create a new uncommitted neuron, and: $N \leftarrow N + 1$.

(9) Go to the step 1, and repeat the Algorithm for the next input.

The flow chart of the SFAM Algorithm is presented in Fig. 4.

## VI. Experimentals

In this study, test arrangement is shown in Fig. 4. as illustrated in Fig 5., there types of partial discharge generation source, corona discharge, surface discharge and internal discharge, were used. Partial discharge signal was measured by using partial discharge detector (OMICRON, model MPD600). Typical measurement results of each partial discharge generation source are illustrated in Fig. 6, Fig. 7 and Fig. 8, respectively.

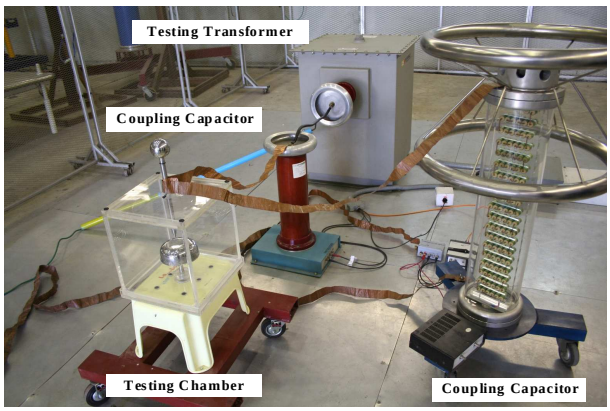


Fig. 5. Test Arrangement.

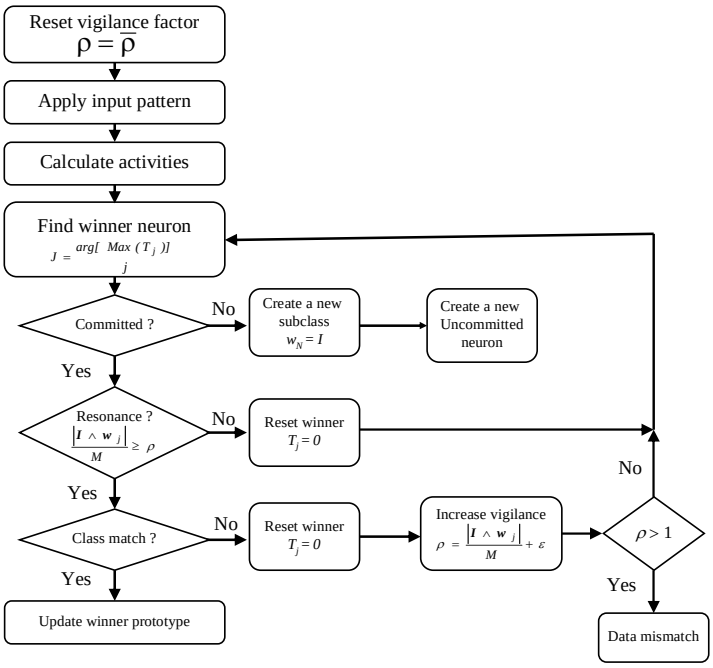


Fig. 4. Flow Chart of the SFAM Training Algorithm for One Input Pattern in One Epoch of Training.

(a) Corona Discharge (b) Surface Discharge (c) Internal Discharge

Fig. 6. Electrode Configuration for Partial Discharge Generation Source.

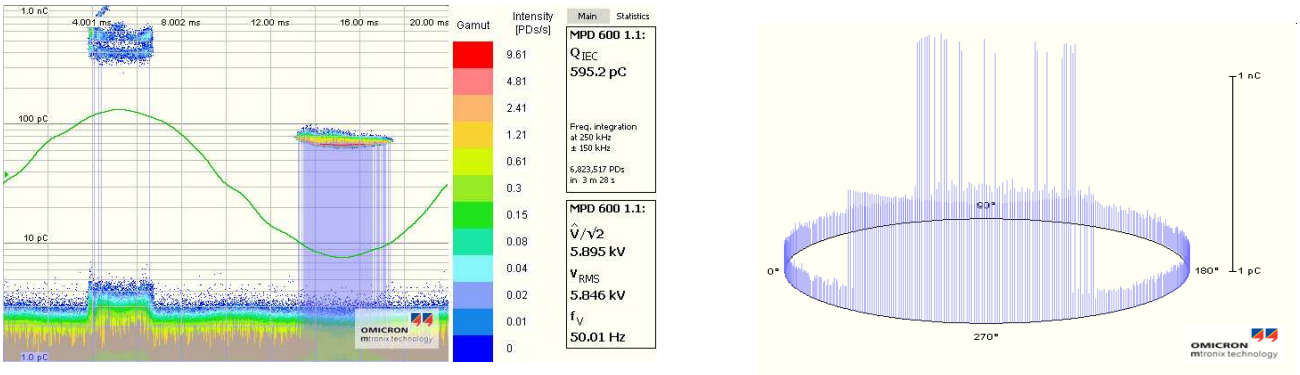


(a) Display on Sinusoidal (b) Display on Elliptical

Fig. 7. Partial Discharge Measurement Result from Corona Discharge

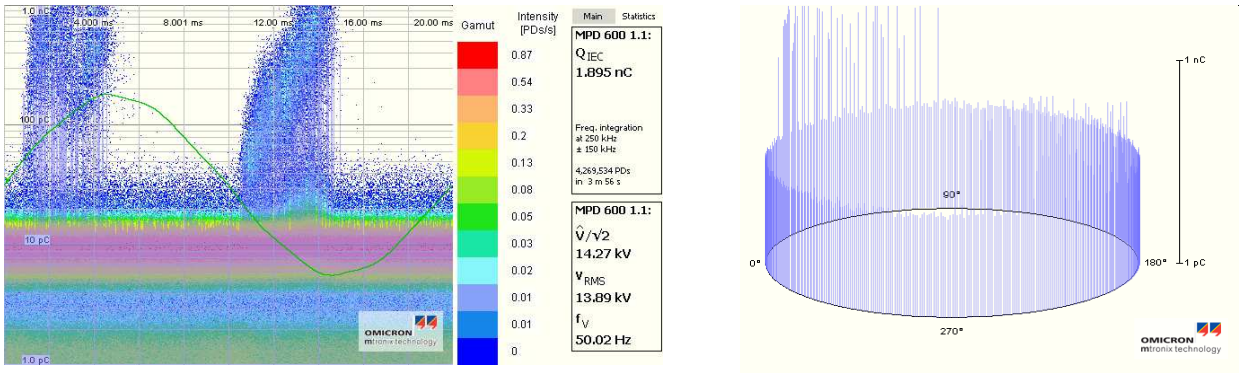


(a) Display on Sinusoidal (b) Display on Elliptical

Fig. 8. Partial Discharge Measurement Result from Surface Discharge

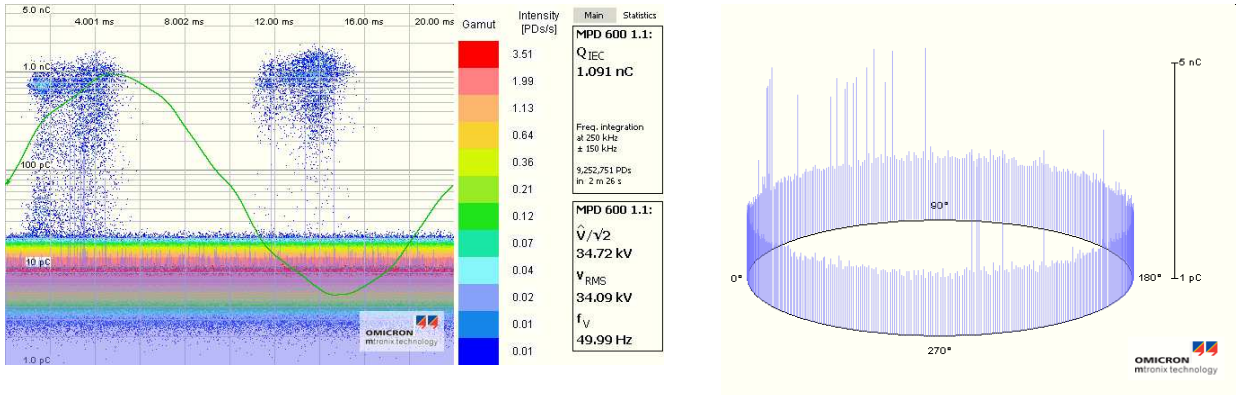


(a) Display on Sinusoidal (b) Display on Elliptical

Fig. 9. Partial Discharge Measurement Result from Internal Discharge

Obviously, differences in pattern of partial discharge measurement results were obtained. Each partial discharge generation source generated individual partial discharge pattern. Then, these measurement data are used to test the purpose technique. Characteristics of partial discharge data were calculated by using statistical tools to apply for pattern recognition and classification. These characteristic of partial discharges include skewness, kurtosis, discharge asymmetry, the cross-correlation factor and modified cross-correlation factor. Characteristics of corona discharge, characteristics of surface discharge and characteristics of internal discharge are showed in Table I, Table II and Table III, respectively. These results were used for pattern recognition and classification.

TABLE I CHARACTERISTICS OF CORONA DISCHARGES

| No. | *Hqn* | | | | *Hn* | | | |
|---|---|---|---|---|---|---|---|---|
| | *Sk+* | *Sk-* | *Ku+* | *Ku-* | *Sk+* | *Sk-* | *Ku+* | *Ku-* |
| 1 | 1.150 | 1.010 | -1.680 | -1.946 | 1.156 | 1.129 | -1.710 | -1.884 |
| 2 | 1.034 | 1.022 | -1.514 | -1.953 | 1.120 | 1.092 | -1.455 | -1.781 |
| 3 | 1.061 | 1.012 | -1.950 | -1.970 | 1.108 | 0.089 | -1.638 | -2.331 |

TABLE II CHARACTERISTICS OF SURFACE DISCHARGES

| No. | *Hqn* | | | | *Hn* | | | |
|---|---|---|---|---|---|---|---|---|
| | *Sk+* | *Sk-* | *Ku+* | *Ku-* | *Sk+* | *Sk-* | *Ku+* | *Ku-* |
| 1 | 1.525 | 1.473 | -0.390 | -0.840 | 1.976 | -0.120 | 1.597 | -2.070 |
| 2 | 1.511 | 1.302 | -0.570 | -0.560 | 1.977 | -0.690 | 1.923 | -2.390 |
| 3 | 1.459 | 1.302 | -0.400 | -1.000 | 1.945 | -0.630 | 1.647 | -2.360 |

TABLE III CHARACTERISTICS OF INTERNAL DISCHARGES

| No. | *Hqn* | | | | *Hn* | | | |
|---|---|---|---|---|---|---|---|---|
| | *Sk+* | *Sk-* | *Ku+* | *Ku-* | *Sk+* | *Sk-* | *Ku+* | *Ku-* |
| 1 | 1.206 | 1.200 | -1.470 | -1.490 | 1.307 | -0.220 | -0.960 | -2.38 |
| 2 | 1.170 | 1.154 | -1.570 | -1.610 | 1.168 | -0.680 | -1.560 | -2.33 |
| 3 | 1.142 | 1.100 | -1.630 | -1.750 | 1.125 | 0.500 | -1.640 | -2.370 |

The existing characteristics of partial discharge signal, illustrated in [4], were used as reference database to train the simplified fuzzy ARTMAP system. Characteristics of reference partial discharge measurement signal (corona discharges, surface discharges and internal discharges) are illustrated in Table IV, Table V and Table VI, respectively.

TABLE IV CHARACTERISTICS OF CORONA DISCHARGES

| No. | *Hqn* | | | | *Hn* | | | |
|---|---|---|---|---|---|---|---|---|
| | *Sk+* | *Sk-* | *Ku+* | *Ku-* | *Sk+* | *Sk-* | *Ku+* | *Ku-* |
| 1 | 1.031 | 1.018 | -1.92 | -1.95 | 1.077 | 0.947 | -1.8 | 2.08 |
| 2 | 1.031 | 10.15 | -1.92 | -1.96 | 1.089 | 1.012 | -1.77 | -1.9 |
| 3 | 1.028 | 1.006 | -1.93 | -1.98 | 1.062 | 0.951 | -1.84 | -0.72 |

TABLE V CHARACTERISTICS OF SURFACE DISCHARGES

| No. | *Hqn* | | | | *Hn* | | | |
|---|---|---|---|---|---|---|---|---|
| | *Sk+* | *Sk-* | *Ku+* | *Ku-* | *Sk+* | *Sk-* | *Ku+* | *Ku-* |
| 1 | 1.493 | 1.471 | -0.26 | -0.28 | 1.918 | -0.46 | 1.451 | -2.3 |
| 2 | 1.496 | 1.45 | -0.27 | -0.39 | 1.954 | -0.59 | 1.702 | -2.35 |
| 3 | 1.486 | 1.454 | -0.34 | -0.41 | 1.919 | -0.54 | 1.408 | -2.35 |

TABLE VI CHARACTERISTICS OF INTERNAL DISCHARGES

| No. | *Hqn* | | | | *Hn* | | | |
|---|---|---|---|---|---|---|---|---|
| | *Sk+* | *Sk-* | *Ku+* | *Ku-* | *Sk+* | *Sk-* | *Ku+* | *Ku-* |
| 1 | 1.115 | 1.153 | -1.71 | -1.6 | 1.11 | -0.37 | -1.73 | -2.39 |
| 2 | 1.141 | 1.152 | -1.63 | -1.6 | 1.113 | -0.43 | -1.71 | -2.39 |
| 3 | 1.133 | 1.153 | -1.66 | -1.58 | 1.124 | -0.63 | -1.68 | -2.34 |

## VII. RESULTS AND DISCISSION

After well training the simplified fuzzy ARTMAP system by our reference PD characteristics, then PD characteristics from the experimental results were inputted to the SFAM system for classify partial discharge generation source. The obtaining results confirmed the effectiveness of purpose technique. The SFAM could correctly recognize and classify partial discharge generation source from PD measurement signal characteristics. The results are showed in table VII.

TABLE VII CLASIFICATION RESULTS BY THE SFAM SYSTEM

| No. test data | Results of classification | |
|---|---|---|
| 1 | corona | correct |
| 2 | corona | correct |
| 3 | corona | correct |
| 4 | surface | correct |
| 5 | surface | correct |
| 6 | surface | correct |
| 7 | internal | correct |
| 8 | internal | correct |
| 9 | internal | correct |

## VIII. CONCLUSIONS

The experimental for partial discharge measurement was conducted. Differences in partial discharge generation source were used in order to characterize partial discharge measurement signal. Characteristics of partial discharge signal were analyzed by using statistical tool and were used to classify partial discharge generation source using the SFAM system. Correctly classification results were obtained. The obtaining results confirmed the effectiveness of the purpose technique, the simplified fuzzy ARTMAP system, to apply for pattern recognition and classification of partial discharge generation source from measurement signal.

## ACKNOWLEDGMENT

The authors would like to thank the high voltage laboratory, Department of Electrical Engineering, Faculty of Engineer, King Mongkut's Institute of Technology, Ladkrabang, Bangkok, Thailand for kind experimental supported.

## REFERENCES

[1] F.H. Kreuger, "*Partial Discharge Detection in High – Voltage Equipment*", Butterworth & Co. (Publishers) Ltd, 1989.

[2] E. Kuffel, W.S. Zaengl and J. Kuffel, "*High Voltage Engineering: Fundamentals*". 2nd, Butterworth – Heinemann, 2000.

[3] B. Marungsri, N. Meeboom and A. Oonsivilai, "Dynamic Model Identification of Induction Motors using Intelligent Search Techniques with taking Core Loss into Account", *WSEAS TRANSACTIONS on POWER SYSTEMS*, Vol. 1, No. 8, August 2006, pp. 1438 – 1445.

[4] A. Oonsivilai and B. Marungsri, "Optimal PID Tuning for AGC system using Adaptive Tabu Search", *Proceedings of the 7th WSEAS International Conference on POWER SYSTEMS*, Beijing, China, September 2007, pp. 42-47.

[5] A. Oonsivilai and B. Marungsri, "Stability Enhancement for Multi-machine Power System by Optimal PID Tuning of Power System Stabilizer using Particle Swarm Optimization", *WSEAS TRANSACTIONS on POWER SYSTEMS*, Issue 5, Volume 3, May 2008, pp. 465 – 474.

[6] A. Oonsivilai and B. Marungsri, "Optimal PID Tuning for Power System Stabilizers Using Adaptive Particle Swarm Optimization Technique", *INTERNATIONAL CONFERENCE ON POWER CONTROL AND OPTIMIZATION: Innovation in Power Control for Optimal Industry. AIP Conference Proceedings*, Volume 1052, July 2008, pp. 116-123

[7] B. Marungsri and A. Oonsivilai, "Partial Discharges Localization in Oil Insulating Transformer using Adaptive Tabu Search", *Proceedings of the 12th WSEAS International Conference on CIRCUITS*, Heraklion, Greece, July 22-24, 2008, pp. 290 – 295.

[8] B. Marungsri and A. Oonsivilai , "Fuzzy ARTMAP Technique for Speech Noise Reduction," *WSEAS International Conference on Signal, Speech and Image Processing*, Beijing, China, pp 20-25, September 2007.

[9] E. Gulski, Computer – Aided Recognition of Partial Discharges using Statistical Tools. Delft University Press,1991.

[10] N.A. Muhamad, B.T. Phung and T.R. Blackburn, "Dissolved Gas Analysis (DGA) of Partial Discharge Fault in Bio-degradable Transformer Insulation Oil", *Universities Power Engineering Conference 2007*.AUPEC 2007, December 2007, pp 1-6.

[11] X. Wang, B. Li, H. T. Roman, O. L. Russo, K. Chin and K. R. Farmer, "Acousto– optical PD Detection for Transformers", *IEEE Transactions on Power Delivery*, Vol. 21, No. 3, July 2006, pp. 1068-1073.

[12] A. Oonsivilai and B. Marungsri, "Application of Artificial Intelligent Technique for Partial Discharges in Oil Insulating Transformer", *WSEAS TRANSACTIONS on SYSTEMS*, Vol.7 No.10, October 2008, pp.920-929.

[13] Y. Lu, X. Tan and X. Hu, "PD detection and localization by acoustic measurements in an oil-filled transformer", *IEEE Science Measurement and Technology*, Vol.147, No.2, March 2000, pp. 81-85.

[14] K. Vicetjindavat, "Pattern Recognition of Partial discharge in High Voltage Equipment", Master Degree Thesis, Chulalongkorn University, 2001.

[15] A. Wichmann, P. Grünewald, and J. Weidner, "Early fault detection inelectrical machines by on-line RF monitoring," *Cigré Symp.*, Vienna,Austria, 1987, pp. 05–87.
[16] J. T. Phillipson, "Experience with RF techniques in the petrochemical industry," *Proc. 4th Int. Conf. Generator and Motor Partial Discharge Testing*, Houston, TX, 1996.
[17] M. D. Judd, L. Yang, and I. B. B. Hunter, "Partial discharge monitoring for power transformers using UHF sensors. Part 1: Sensors and signal interpretation," *IEEE Electr. Insul. Mag.*, Vol. 21, No. 1, Mar./Apr. 2005, pp. 5-14.
[18] S. Grossberg, "Adaptive pattern classification and universal recoding, II: feedback, expectation,olfaction and illusions", *Biological Cybernetics*, Vol. 23, 1976, pp. 187–202.
[19] G. A. Carpenter and S. Grossberg, "ART2: Self-organization of stable category recognition codes for analog input patterns", *Applied Optics*, vol. 26, No. 23, 1987, pp. 4919– 4930.
[20] G. A. Carpenter and S. Grossberg, "ART3: Hierarchical search using chemical transmitters in self-organizing pattern recognition architecture, *Neural Networks*, Vol.3, 1990, pp. 129–152.
[21] G. A. Carpenter, G. S. Grossberg and J. H.Reynolds, "ARTMAP: Supervised real-time learning and classification of mon-stationary data by a self-organizing neural network", *Neural Networks*, Vol. 4, 1991, pp. 565–588.
[22] G. A. Carpenter, G. S. Grossberg and D. B. Rosen, "Fuzzy ART: Fast stable learning and categorization of analog patterns by an adaptive resonance system", *Neural Networks*, Vol. 4, 1991, pp. 759–771.
[23] G. A. Carpenter, S. Grossberg, N. Markuzon, J. H. Reynolds, and D. B. Rosen, "Fuzzy ARTMAP: A neural network architecture for incremental supervised learning of analog multidimensional maps", *IEEE Trans. on Neural Networks*, Vol.3, No. 5, 1992, pp. 698–713.
[24] T. Kasuba, "Simplified Fuzzy ARTMAP", *AI Expert*, Vol. 8, No. 11, 1993, pp.18–25.
[25] M. Vakil-Gahimisheh and N. Pavešić, "A Fast Simplified Fuzzy ARTMAP Network", *Neural Processing Letters*, Vol. 17, 2003, pp. 273–316.

**Suphachai Boonpoke** was born in Surin Province, Thailand, in 1984. He received his B. Eng. in Electrical Engineering from Suranaree University of Technology, Nakhon Ratchasima, Thailand, in 2005. Recently, he is a graduate student in School of Electrical Engineering, Suranaree University of Technology. His research interesting area is high voltage insulation technology.

**Boonruang Marungsri,** was born in Nakhon Ratchasima Province, Thailand, in 1973. He received his B. Eng. and M. Eng. from Chulalongkorn University, Thailand in 1996 and 1999 and D. Eng. from Chubu University, Kasugai, Aichi, Japan in 2006, all in electrical engineering, respectively. Dr. Marungsri is currently an assistant professor in School of Electrical Engineering, Suranaree University of Technology, Thailand. His areas of interest are high voltage insulation technologies and electrical power system.